Journal of Magnetism and Magnetic Materials 323 (2011) 163–166

Contents lists available at ScienceDirect

Journal of Magnetism and Magnetic Materials

journal homepage: www.elsevier.com/locate/jmmm

Effect of film morphology on the magnetic properties for Nd–Fe–B thin films

T. Sato [a], H. Kato [b], T. Shima [b,*], Y.K. Takahashi [c], K. Hono [c]

[a] Toyota Central R&D Labs Inc., 41-1, Yokomichi, Nagakute, Aichi 480-1192, Japan
[b] Faculty of Engineering, Tohoku Gakuin University, 1-13-1, Chuo, Tagajo 985-8537, Japan
[c] Magnetic Materials Center, National Institute for Materials Science, 1-2-1 Sengen, Tsukuba 305-0047, Japan

ARTICLE INFO

Article history:
Received 12 June 2010
Received in revised form
25 August 2010
Available online 8 September 2010

Keywords:
High coercivity material
Morphology
Nd–Fe–B thin film
Perpendicular anisotropy
Nano-structure

ABSTRACT

The microstructure and magnetic properties of Nd–Fe–B thin films with a particulate structure were investigated. The nominal thickness of the Nd–Fe–B layer (t_N) was varied from 2 to 50 nm on a (0 0 1) Mo buffer layer. The films were grown with their *c*-axis perpendicular to the plane, and the morphology of the film with t_N=2 nm was shown to be particulate from an atomic force microscope image. The slope of the initial magnetization curve became steeper by increasing the t_N value in the initial magnetization curve, indicating that the film morphology composed of single domain particles changed to that of multi-domain particles with growth. The film with t_N=8 nm, which had a structure consisting of a mixture of single and multiple domain particles, showed the maximum value of the coercivity measured in the direction perpendicular to the film plane (H_c) as 19.5 kOe.

1. Introduction

$Nd_2Fe_{14}B$ alloy [1] has been used widely as a magnetomotive force in applications such as motors, actuators, and sensors for its large magnetocrystalline anisotropy ($K_{u1}=4.5\times10^6$ J/m^3 at room temperature) and relatively high magnetization (M_s=1.6 T) [2]. Recently, the consumption of Nd–Fe–B sintered magnets has increased due to the expansion in the market for hybrid vehicles (HVs) resulting from environmental and energy issues. One critical issue must be resolved to sustain the supply of high performance permanent magnets for HVs, i.e., the indispensable addition of heavy rare earth elements such as Tb and Dy to the Nd–Fe–B sintered magnet for the enhancement of coercivity at high temperature utilization [3,4]. This issue results from the sudden increase in the price of these heavy rare earth elements due to the scarce natural resources of these elements. Consequently, the reduction of these elements from the Nd–Fe–B permanent magnet becomes necessary. The actual value of coercivity of commercial Nd–Fe–B sintered magnets is much lower than the theoretically predicted one [5], and the reason for the discrepancy between them has not been clarified yet. Therefore, the elucidation of the coercivity mechanism is essential for reducing the amount of heavy rare earth elements from the Nd–Fe–B magnets [6–14]. The present study demonstrates that by changing the nominal thickness of Nd–Fe–B films, film morphology can be varied from isolated small particles to continuous structures. The improvement in coercivity of small particles was also investigated to understand the intrinsic coercivity of Nd–Fe–B magnets.

2. Experimental

Nd–Fe–B films were prepared by co-sputtering Fe, $Fe_{80}B_{20}$ (at%) and Nd targets using an UHV-compatible dc magnetron sputtering system (base pressure$\sim1\times10^{-8}$ Pa). A Cr seed layer of 1 nm and an epitaxial Mo buffer layer of 20 nm were deposited onto the MgO (1 0 0) single crystal substrate at room temperature (RT). Then, the substrates were heated to 625°C during the deposition of the Nd–Fe–B layer. A Cr layer of 10 nm was deposited at R.T. at the end as an oxidation protection layer. The nominal thickness of the Nd–Fe–B film (t_N) varied in the range of 2–50 nm, and it was calculated as the product of the deposition rate of 0.04 nm/s and the deposition time. The composition of the Nd–Fe–B layer was determined to be $Nd_{15.2}Fe_{70.2}B_{14.6}$ (at%) by electron probe X-ray microanalysis (EPMA). Structural analysis was performed by X-ray diffraction (XRD) with Cu Kα radiation, atomic force microscopy (AFM) and transmission electron microscopy (TEM). Elemental distribution in the film was examined by energy filtering TEM (EF-TEM) with a Gatan TREDIUM imaging filter. The magnetization curves were measured by a superconducting quantum interference device (SQUID) magnetometer in the field up to 55 kOe. All the measurements were carried out at room temperature.

3. Results and discussion

The X-ray diffraction patterns for the films with various values of t_N=2 nm(a), 5 nm(b), 8 nm(c), 10 nm(d), 20 nm(e), and 50 nm(f) are shown in Fig. 1. The sharp diffraction peaks denoted by the asterisks are due to the MgO (1 0 0) substrate, and the peak

* Corresponding author.
E-mail address: shima@tjcc.tohoku-gakuin.ac.jp (T. Shima).

0304-8853/$ - see front matter © 2010 Elsevier B.V. All rights reserved.
doi:10.1016/j.jmmm.2010.08.056

from the Mo (2 0 0) is also observed clearly at around $2\theta=58.6^\circ$ for all the films. The peak observed at $2\theta=65.2^\circ$ is identified as the one from Fe (2 0 0) for the film with $t=2$ nm. Meanwhile, the peaks from $Nd_2Fe_{14}B$ (0 0 4) and (0 0 1 0) mainly appeared at 29.3° and 78.3° for the films with $t\geq 5$ nm. The intensity of the peaks from $Nd_2Fe_{14}B$ became stronger with increase in t. These diffraction patterns indicate that the orientation relationship among the substrate and each layer is MgO (1 0 0)∥Mo (1 0 0)∥$Nd_2Fe_{14}B$ (0 0 1). However, the peaks from $Nd_{1+\varepsilon}Fe_4B_4$ (2 0 0) and Nd (0 0 4) began to appear at 25.0° and 30.3° for the films with $t=20$ and 50 nm.

AFM images of the films with different t_N are shown in Fig. 2. The films with $t_N=2$ and 5 nm were grown with the island growth mode. The typical lateral size of the particle was in the range 20–100 nm. A remarkable change in the morphology of the film was observed for $t_N=5$–20 nm, i.e., the film morphology changed from a particulate to a continuous structure by the growth of $Nd_2Fe_{14}B$ particles.

Cross-sectional TEM image of the film with $t=5$ nm is shown in Fig. 3. The stacking of the c-plane of the tetragonal $Nd_2Fe_{14}B$ structure was clearly observed, indicating that the c-axis of the $Nd_2Fe_{14}B$ alloy is perpendicular to the film plane. However, the interface between the Mo layer and the Nd–Fe–B layer was not clear. This may have been caused by the strain effect. In-plane bright field TEM image and the energy filtered element maps of Fe and Nd for the film with $t=5$ nm are shown in Fig. 4. The in-plane bright field image (a) indicates that the film was not grown continuously but formed isolated particles, which was previously demonstrated in the AFM image (Fig. 2 (b)). The elemental maps of Fe (b) and Nd (c) show that most of the islands composed of a high concentration of the Fe region and a moderate concentration of the Nd region, indicating the formation of the $Nd_2Fe_{14}B$ alloy. The region with the brighter contrast in the Nd map (one marked with a white arrow) is thought to be a Nd-rich phase. In the Fe distribution map, the black region with low Fe concentration is observed whereas a brighter contrast was observed in the Nd map. This indicates the formation of the Nd-rich region, since the composition of both Nd and B was higher in the film than that in the stoichiometric concentration of the $Nd_2Fe_{14}B$ compound. This region is thought to be the $Nd_{1+\varepsilon}Fe_4B_4$ phase from the XRD profiles.

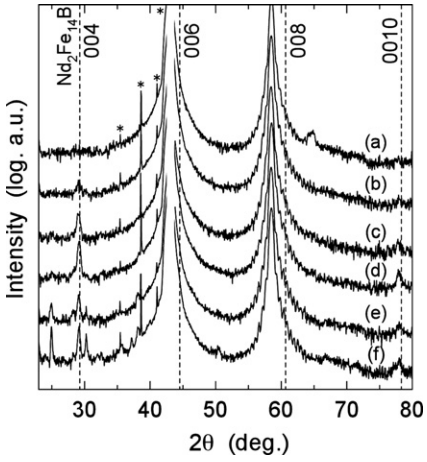

Fig. 1. X-ray diffraction patterns for the Nd–Fe–B films with various nominal thicknesses ($t=2$ nm (a), 5 nm (b), 8 nm (c), 10 nm (d), 20 nm (e), and 50 nm (f)). Asterisks denote the peak from the MgO (1 0 0) single crystal substrate.

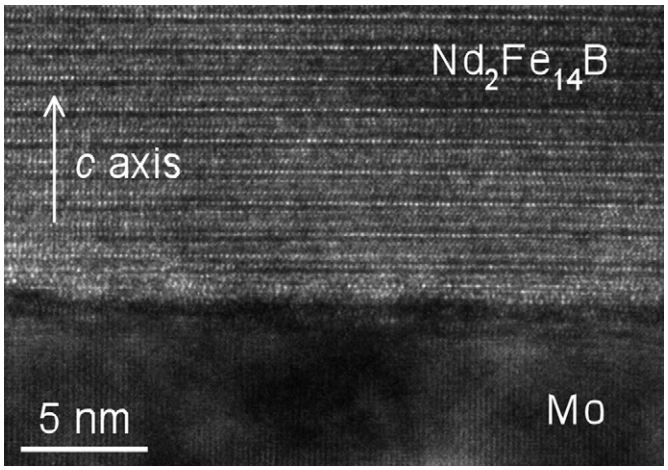

Fig. 3. Cross-sectional TEM image of the Nd–Fe–B film with $t=5$ nm.

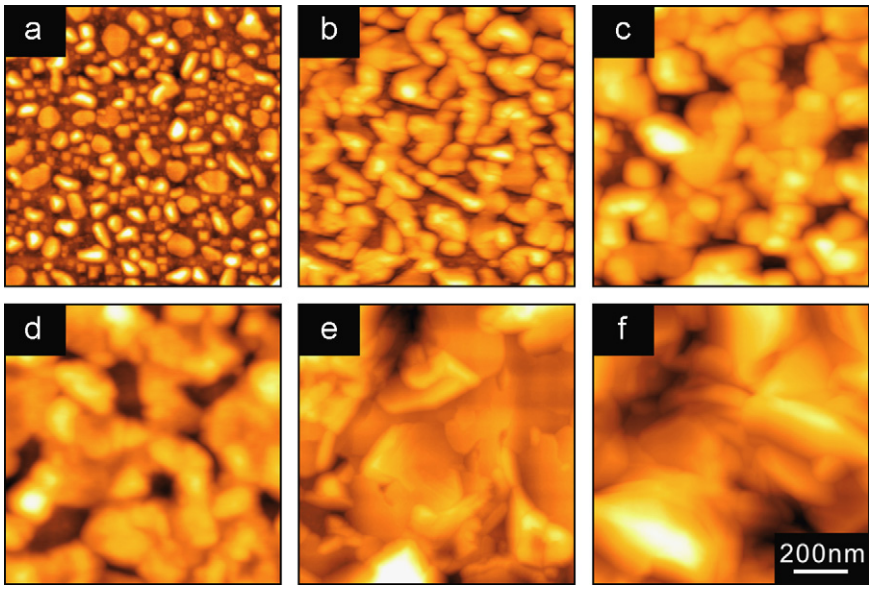

Fig. 2. AFM images of the Nd–Fe–B films with various film thicknesses ($t=2$ nm (a), 5 nm (b), 8 nm (c), 10 nm (d), 20 nm (e), and 50 nm (f)).